



A has three carbonyl groups and five carbons with double-bond chemical shifts, one of the resonances ( $\delta_C$  173.6 or 173.5) in the carbonyl region must be a highly deshielded double-bond carbon. Therefore, the eight degrees of unsaturation were explained as three carbonyl groups and three double bonds, indicating that formicin A has a bicyclic structure.

An array of COSY couplings identified from the terminal methyl group protons ( $H_3$ -16) to the  $H_2$ -13 assigned an aliphatic chain. The  $H_2$ -1'/ $H_2$ -2' correlation elucidated a short spin system composed of two connected methylenes flanked by heteroatoms (Figure 1). A series of COSY couplings of H-2

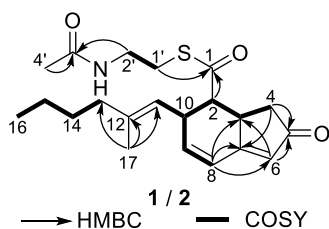


Figure 1. Key COSY and HMBC couplings of 1 and 2.

to H-4 and H-8 to H-11, as well as the H-2/H-10 COSY cross peak, were used to construct the seven-carbon spin system. This partial structure was further extended to C-7 ( $\delta_C$  173.6) and C-6 ( $\delta_C$  126.5) based on HMBC couplings from H-8 to C-7 and C-6. The H-6/C-5 and  $H_2$ -4/C-5 HMBC couplings located the C-5 ( $\delta_C$  210.7) ketone group between C-4 and C-6. A detailed analysis of the H-8/H-9 coupling constant (9.9 Hz) indicated that these protons belong to a six-membered alkene. The cyclic hexene moiety was elucidated by three-bond heteronuclear correlations from H-8 to C-3. In addition, the H-6/C-3 and  $H_2$ -4/C-7 HMBC couplings confirmed the existence of a cyclopropanone, thus revealing the bicyclic indenone structure in 1.

The C-13 to C-16 hydrocarbon chain was then connected to C-12 by HMBC couplings from  $H_3$ -17 to C-11, C-12, and C-13. The C-3' ( $\delta_C$  173.5) was situated between C-2' and C-4' based on the  $H_2$ -2'/C-3' and  $H_3$ -4'/C-3' heteronuclear correlations. The last unused carbon ( $\delta_C$  199.3) and the sulfur comprised a thioester functional group based on the carbon chemical shift, which was assigned between C-2 and C-1' by HMBC coupling from H-2 and  $H_2$ -1' to C-1, assembling *N*-acetylcysteamine and completing the structure of formicin A (1). The structure of 1 was further supported by MS/MS fragments (Figure 2 and Figure S2). The geometry of the double bond in the chain was determined to be 11*E* by the H-11/ $H_2$ -13 ROESY correlation.

Formicin B (2) was isolated as a white powder. The molecular formula was established as  $C_{21}H_{29}NO_3S$  based on the analysis of HR-ESI mass spectrometry ( $[M + Na]^+$  at  $m/z$  398.1776, calculated 398.1760). The molecular formula of 2 is identical to that of 1. The  $^1H$  and  $^{13}C$  NMR spectra of 2 were highly similar to those of 1 (Table 1). Combined 2D NMR

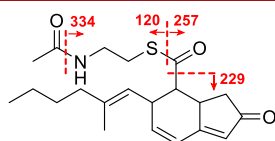


Figure 2. ESI-HR-MS/MS fragmentation of 1.

analyses disclosed that the planar structure of 2 is identical to that of 1. A careful comparison of the  $^1H$  and  $^{13}C$  NMR data of 1 and 2 revealed notable differences in the  $^1H$ - $^1H$  coupling constant at H-2 (dd,  $J = 12.7, 5.4$  Hz for 2) and  $^{13}C$  chemical shifts at C-2 and C-4 ( $\delta_C$  58.2 and 42.2, respectively, for formicin B), suggesting that 2 is a diastereomer of 1 with modifications around these carbons.

The relative configurations of 1 and 2 were established by analyzing the ROESY NMR data (Figure 3). Formicin A showed H-3/H-2, H-3/H-4a, and H-3/H-11 ROESY correlations, indicating that H-2 ( $\delta_H$  3.13), H-3 ( $\delta_H$  3.38), H-4a ( $\delta_H$  2.57), and H-11 ( $\delta_H$  5.25) are positioned on the same side. Therefore, the relative configuration of 1 was determined to be 2*S*\*, 3*S*\*, and 10*S*\*. The H-2 of 2 clearly possesses axial-axial coupling ( $J = 12.7$  Hz) with H-3. The H-3/H-4a and H-3/H-11 ROESY correlations positioned H-3 ( $\delta_H$  3.48), H-4a ( $\delta_H$  2.72), and H-11 ( $\delta_H$  5.04) on the same side. On the contrary, the H-2/H-4b ROESY cross-peaks determined that H-2 is on the opposite side, thus establishing the 2*R*\*, 3*S*\*, and 10*S*\* configuration.

Formicin C (3) was purified as a white powder, and its molecular formula was determined to be  $C_{17}H_{22}O_3$  based on  $^1H$  and  $^{13}C$  NMR spectroscopy and HR-ESI mass spectrometry ( $[M + H]^+$  at  $m/z$  275.1638, calculated 275.1641). The  $^1H$  and  $^{13}C$  NMR spectra of 3 are simpler than those of 1 and 2 without the signals originating from the *N*-acetylcysteamine thioester (SNAC). In addition, the thioester carbons around  $\delta_C$  200 ppm disappeared, and a carbon at  $\delta_C$  176.7 was observed. The  $\alpha$ -carbon of the thioester was upfield-shifted from  $\delta_C$  56–59 to  $\delta_C$  51.0, also supporting the above-mentioned modification in 3 relative to 1 and 2. Further analysis of 1D and 2D NMR spectra, considering seven degrees of double-bond equivalents, elucidated the structure of 3, which contains a carboxylic acid moiety instead of SNAC.

ROESY correlations and  $^1H$ - $^1H$  coupling constants around the stereogenic centers C-2, C-3, and C-10 in 3 were analogous to those in 2 but obviously different from 1. Careful examination of these spectroscopic data determined the relative configuration of formicin C (3) as 2*R*\*, 3*S*\*, and 10*S*\* (Figure S27), which is identical to 2. To determine the absolute configurations of formicin C (3), the carboxylic acid attached to C-2 was derivatized using the phenylglycine methyl ester (PGME) method.<sup>12</sup>  $\Delta\delta_{S-R}$  values of *S*- and *R*-PGME esters (3a and 3b, respectively) were calculated based on their  $^1H$  and COSY NMR data. As a result, the absolute configuration of C-2 was determined to be *R* (Figure S28). Therefore, the other chiral centers were subsequently established as 3*S* and 10*S*.

Formicins A and B do not have a functional group for chiral derivatization to establish their absolute configurations. Electronic circular dichroism (ECD) spectra could not clearly distinguish the diastereomers with the opposite C-2 configurations (Figures S3 and S4). Therefore, formicin C (3) with the established absolute configuration *vide supra* was derivatized with *N*-acetylcysteamine to generate formicin B (Figure 4). This synthetic formicin B (2a) was identical to natural formicin B (2), as assessed by  $^1H$  and  $^{13}C$  NMR (Figures S35 and S36). The optical rotation of 2a was also identical to that of 2. Thus the absolute configuration of 2 was deemed to be 2*R*, 3*S*, and 10*S*. Accordingly, the absolute configuration of formicin A (1) was deduced as 2*S*, 3*S*, and 10*S*.

Table 1.  $^1\text{H}$  (800 MHz) and  $^{13}\text{C}$  (200 MHz) NMR Data of Formicins A–C (1–3) in  $\text{CD}_3\text{OD}$ 

position	formicin A (1)		formicin B (2)		formicin C (3)	
	$\delta_{\text{C}}$ , type	$\delta_{\text{H}}$ , mult ( <i>J</i> in Hz)	$\delta_{\text{C}}$ , type	$\delta_{\text{H}}$ , mult ( <i>J</i> in Hz)	$\delta_{\text{C}}$ , type	$\delta_{\text{H}}$ , mult ( <i>J</i> in Hz)
1	199.3, C		199.8, C		176.7, C	
2	56.7, CH	3.13, br d (5.2)	58.2, CH	3.16, dd (12.7, 5.4)	51.0, CH	2.75, dd (13.0, 5.4)
3	37.3, CH	3.38, m	37.1, CH	3.48, m	37.6, CH	3.33, m
4a	40.0, $\text{CH}_2$	2.57, dd (18.2, 6.8)	42.2, $\text{CH}_2$	2.72, dd (18.2, 6.4)	43.3, $\text{CH}_2$	2.81, dd (18.6, 6.3)
4b		2.24, dd (18.2, 4.1)		2.06, dd (18.2, 4.0)		2.09, dd (18.6, 4.0)
5	210.7, C		210.4, C		211.3, C	
6	126.5, CH	5.90, d (1.8)	126.9, CH	5.93, d (1.9)	126.4, CH	5.90, d (1.9)
7	173.6, C		174.3, C		175.3, C	
8	123.5, CH	6.67, d (9.9)	122.6, CH	6.63, d (9.6)	122.6, CH	6.62, d (9.6)
9	140.7, CH	6.15, dd (9.9, 5.9)	142.1, CH	6.20, dd (9.6, 5.6)	143.2, CH	6.24, dd (9.6, 5.8)
10	40.7, CH	3.65, dd (9.2, 5.9)	40.6, CH	3.88, ddd (10.2, 5.6, 5.4)	39.5, CH	3.83, ddd (10.0, 5.8, 5.4)
11	123.5, CH	5.25, dq (9.2, 0.9)	119.5, CH	5.04, dq (10.2, 1.1)	120.2, CH	5.12, dq (10.0, 1.0)
12	141.1, C		141.4, C		141.2, C	
13	40.4, $\text{CH}_2$	2.08, t (7.7)	40.6, $\text{CH}_2$	2.00, t (7.4)	40.8, $\text{CH}_2$	2.02, t (7.4)
14	31.2, $\text{CH}_2$	1.44, tt (7.7, 7.5)	31.1, $\text{CH}_2$	1.36, tt (7.5, 7.4)	31.2, $\text{CH}_2$	1.40, tt (8.1, 7.4)
15	23.4, $\text{CH}_2$	1.32, m	23.2, $\text{CH}_2$	1.26, m	23.3, $\text{CH}_2$	1.29, m
16	14.3, $\text{CH}_3$	0.93, t (7.4)	14.3, $\text{CH}_3$	0.90, t (7.4)	14.3, $\text{CH}_3$	0.90, t (7.3)
17	16.7, $\text{CH}_3$	1.82, d (0.9)	16.7, $\text{CH}_3$	1.73, d (1.1)	16.5, $\text{CH}_3$	1.74, d (1.0)
1'	29.4, $\text{CH}_2$	2.98, m	28.8, $\text{CH}_2$	2.99, m		
2'	39.9, $\text{CH}_2$	3.30, td (6.5, 1.0)	40.2, $\text{CH}_2$	3.27, td (7.0, 2.6)		
3'	173.5, C		173.4, C			
4'	22.5, $\text{CH}_3$	1.89, s	22.5, $\text{CH}_3$	1.92, s		

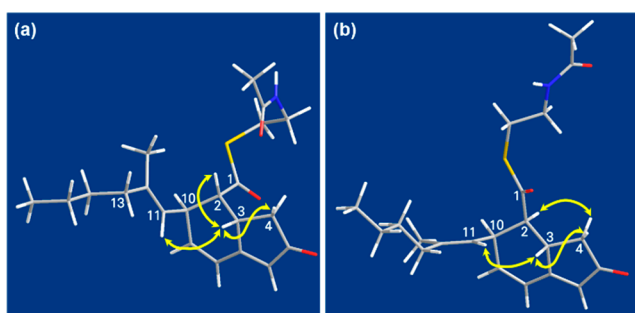


Figure 3. Key ROESY correlations of (a) 1 and (b) 2.

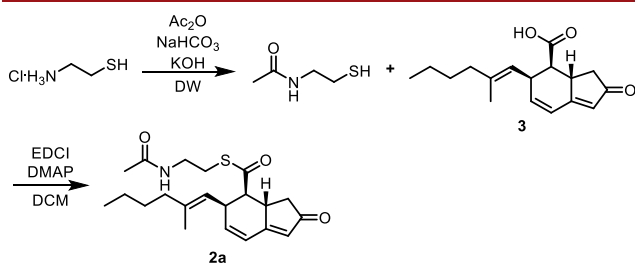


Figure 4. Thioesterification of 3 to yield 2.

To discover biological activities of formicins A–C (1–3), we first determined their antiproliferative activity against human triple-negative breast cancer (TNBC) cells. As shown in Figure 5a, only formicin A (1) exhibited significant antiproliferative activity in a concentration-dependent manner against MDA-MB-231 human TNBC cells. We also found that formicin A exhibited more selective antiproliferative activity against TNBC cells compared with human normal lung fibroblast cells (MRC-5) (Figure S40 and Table S1).

Liver kinase B1 (LKB1) is a tumor suppressor in many cancers including breast cancer. A recent study revealed that

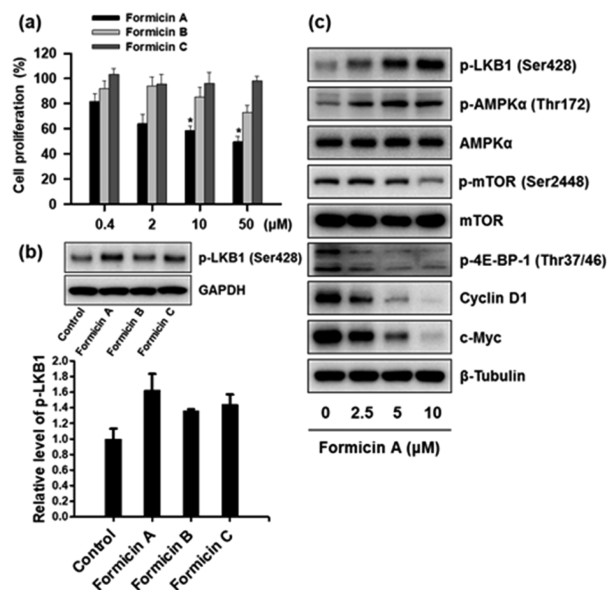


Figure 5. (a) MDA-MB-231 human TNBC cells were incubated with the indicated concentrations of formicins A–C for 72 h; then, the cell proliferation was measured using a sulforhodamine B (SRB) assay. Data are expressed as means  $\pm$  SD from three independent experiments. \* $p < 0.05$  indicates significant difference relative to the vehicle-treated control group. (b) MDA-MB-231 human TNBC cells were incubated with formicins A–C (test concentration: 5  $\mu\text{M}$ ) for 24 h; then, the level of p-LKB1 was measured using Western blot analysis. GAPDH was used as an internal control. The relative intensity of p-LKB1 was quantified using NIH ImageJ software. (c) Levels of LKB1/AMPK signaling pathway proteins were detected by Western blot analysis.  $\beta$ -Tubulin was used as an internal control.

low expression levels of LKB1 are highly associated with poor clinical outcomes of triple-negative breast cancer patients.<sup>13</sup> LKB1 directly phosphorylates and activates adenosine mono-

phosphate-activated protein kinase (AMPK) to regulate the cellular functions of human cancer cells, including metabolism, autophagy, and growth.<sup>14–16</sup> Therefore, we evaluated the effect of 1–3 on the activation of LKB1 in TNBC cells. Consistent with its antiproliferative activity, formicin A (1) exhibited the most potent stimulatory effect on LKB1 activation (phospho-LKB1) (Figure 5b). Because LKB1 phosphorylates AMPK and downregulates its downstream targets,<sup>14–16</sup> we next explored whether formicin A (1) affects the AMPK signaling pathway. As shown in Figure 5c, formicin A significantly increased AMPK phosphorylation (p-AMPK) via LKB1 activation and then subsequently downregulated the expression of AMPK-mediated downstream target proteins, including phosphomammalian target of rapamycin (p-mTOR), phosphoeukaryotic translation initiation factor 4E-binding protein 1 (p-4E-BP-1), cyclin D1, and c-Myc. Taken together, these data demonstrate that formicin A is able to suppress the proliferation of human TNBC cells by regulating the LKB1-mediated AMPK signaling pathway.

Containing an indenone core, formicins are structurally unique. This [4.3.0] bicyclic scaffold with a diene conjugated with a ketone in the five-membered ring has been rarely reported in nature. The only examples are brasilane A from the fungus *Aspergillus terreus*<sup>17</sup> and tundrenone from *Methylobacter tundripaludum*.<sup>18</sup> Brasilane A, a sesquiterpenoid, is obviously biosynthesized through a terpenoid pathway.<sup>17</sup> Bioinformatic analysis of *M. tundripaludum* revealed that indenone is derived from chorismate in this bacterium.<sup>18</sup> However, because C-2 is an epimeric center in 1–3, the indenone moiety in the formicins could have originated from a polyketide-derived chain with a branched methyl group (C-17) through cyclization. The *N*-acetylcysteamine thioester (SNAC) is another interesting component. SNACs are widely used to mimic the phosphopantetheine termini of acyl carrier proteins and peptidyl carrier proteins in studies of polyketide and nonribosomal peptide biosynthesis.<sup>19</sup> However, *N*-acetylcysteamine is extremely rare as a component of natural metabolites. *Streptomyces* spp. produced epithienamycins, antibiotics bearing an *N*-acetylcysteamine bound at a double-bond carbon in their carbapenem ring.<sup>20</sup> However, the only precedent natural compounds incorporating SNACs are parathiosteroids A–C from a soft coral *Paragorgia* sp. collected in Madagascar.<sup>21</sup>

To the best of our knowledge, formicins are the first natural compounds containing the combination of the rare structural motifs, indenone and *N*-acetylcysteamine. As a new bioactive scaffold, formicin A (1) regulates the LKB1-mediated AMPK signaling pathway and resultantly inhibits the proliferation of human TNBC cells. Moreover, the discovery of formicins provides support that ant-associated bacteria are a prolific chemical reservoir of structurally novel bioactive compounds.

## ■ ASSOCIATED CONTENT

### SI Supporting Information

The Supporting Information is available free of charge at <https://pubs.acs.org/doi/10.1021/acs.orglett.0c01584>.

Full experimental procedures, HR-MS/MS spectra of 1 and 2, experimental and calculated ECD spectra of 1–3, 1D and 2D NMR spectra of 1–3, and antiproliferative effects of 1 (PDF)

## ■ AUTHOR INFORMATION

### Corresponding Author

**Dong-Chan Oh** – Natural Products Research Institute, College of Pharmacy, Seoul National University, Seoul 08826, Republic of Korea; [orcid.org/0000-0001-6405-5535](https://orcid.org/0000-0001-6405-5535);  
Email: [dongchanoh@snu.ac.kr](mailto:dongchanoh@snu.ac.kr)

### Authors

**Young Eun Du** – Natural Products Research Institute, College of Pharmacy, Seoul National University, Seoul 08826, Republic of Korea

**Woong Sub Byun** – Natural Products Research Institute, College of Pharmacy, Seoul National University, Seoul 08826, Republic of Korea

**Seok Beom Lee** – Research Institute of Pharmaceutical Science and College of Pharmacy, Seoul National University, Seoul 08826, Republic of Korea

**Sunghoon Hwang** – Natural Products Research Institute, College of Pharmacy, Seoul National University, Seoul 08826, Republic of Korea

**Yern-Hyerk Shin** – Natural Products Research Institute, College of Pharmacy, Seoul National University, Seoul 08826, Republic of Korea

**Bora Shin** – Natural Products Research Institute, College of Pharmacy, Seoul National University, Seoul 08826, Republic of Korea

**Yong-Joon Jang** – Natural Center of Life and Environment, Seoul 08826, Republic of Korea

**Suckchang Hong** – Research Institute of Pharmaceutical Science and College of Pharmacy, Seoul National University, Seoul 08826, Republic of Korea

**Jongheon Shin** – Natural Products Research Institute, College of Pharmacy, Seoul National University, Seoul 08826, Republic of Korea; [orcid.org/0000-0002-7536-8462](https://orcid.org/0000-0002-7536-8462)

**Sang Kook Lee** – Natural Products Research Institute, College of Pharmacy, Seoul National University, Seoul 08826, Republic of Korea; [orcid.org/0000-0002-4306-7024](https://orcid.org/0000-0002-4306-7024)

Complete contact information is available at:  
<https://pubs.acs.org/10.1021/acs.orglett.0c01584>

### Notes

The authors declare no competing financial interest.

## ■ ACKNOWLEDGMENTS

This work was supported by the National Research Foundation of Korea Grants funded by the Korean Government (Ministry of Science, ICT and Future Planning) (2018R1A4A1021703).

## ■ REFERENCES

- (1) Chevrette, M. G.; Carlson, C. M.; Ortega, H. E.; Thomas, C.; Ananiev, G. E.; Barns, K. J.; Book, A. J.; Cagnazzo, J.; Carlos, C.; Flanigan, W.; Grubbs, K. J.; Horn, H. A.; Hoffmann, F. M.; Klassen, J. L.; Knack, J. J.; Lewin, G. R.; McDonald, B. R.; Muller, L.; Melo, W. G. P.; Pinto-Tomas, A. A.; Schmitz, A.; Wendt-Pienkowski, E.; Wildman, S.; Zhao, M.; Zhang, F.; Bugni, T. S.; Andes, D. R.; Pupo, M. T.; Currie, C. R. *Nat. Commun.* **2019**, *10*, 1–11.
- (2) Grimaldi, D.; Engel, M. S. *Evolution of the Insects*; Cambridge University Press: Cambridge, U.K., 2005; p. 147.
- (3) Currie, C. R.; Scott, J. A.; Summerbell, R. C.; Malloch, D. *Nature* **1999**, *398*, 701–704.
- (4) Oh, D.-C.; Poulsen, M.; Currie, C. R.; Clardy, J. *Nat. Chem. Biol.* **2009**, *5*, 391–393.

- (5) Carr, G.; Derbyshire, E. R.; Caldera, E.; Currie, C. R.; Clardy, J. *J. Nat. Prod.* **2012**, *75*, 1806–1809.
- (6) Shin, B.; Park, S. H.; Kim, B.-Y.; Jo, S.-I.; Lee, S. K.; Shin, J.; Oh, D.-C. *J. Nat. Prod.* **2017**, *80*, 2910–2916.
- (7) Hong, S.-H.; Ban, Y. H.; Byun, W. S.; Kim, D.; Jang, Y.-J.; An, J. S.; Shin, B.; Lee, S. K.; Shin, J.; Yoon, Y. J.; Oh, D.-C. *J. Nat. Prod.* **2019**, *82*, 903–910.
- (8) Chang, P. T.; Rao, K.; Longo, L. O.; Lawton, E. S.; Scherer, G.; Van Arnam, E. B. *J. Nat. Prod.* **2020**, *83*, 725–729.
- (9) Radchenko, A. *Ann. Zool.* **2005**, *55*, 127–221.
- (10) Ramalho, M. O.; Bueno, O. C.; Moreau, C. S. *BMC Evol. Biol.* **2017**, *17*, 96.
- (11) Sit, C. S.; Ruzzini, A. C.; Van Arnam, E. V.; Ramadhar, T. R.; Currie, C. R.; Clardy, J. *Proc. Natl. Acad. Sci. U. S. A.* **2015**, *112*, 13150–13154.
- (12) Yabuuchi, T.; Kusumi, T. *J. Org. Chem.* **2000**, *65*, 397–404.
- (13) Rhodes, L. V.; Tate, C. R.; Hoang, V. T.; Burks, H. E.; Gilliam, D.; Martin, E. C.; Elliott, S.; Miller, D. B.; Buechlein, A.; Rusch, D.; Tang, H.; Nephew, K. P.; Burow, M. E.; Collins-Burow, B. M. *Oncogenesis* **2015**, *4*, e168.
- (14) Shaw, R. J.; Bardeesy, N.; Manning, B. D.; Lopez, L.; Kosmatka, M.; DePinho, R. A.; Cantley, L. C. *Cancer Cell* **2004**, *6*, 91–99.
- (15) Momcilovic, M.; Shackelford, D. B. *Br. J. Cancer* **2015**, *113*, 574–584.
- (16) Faubert, B.; Vincent, E. E.; Griss, T.; Samborska, B.; Izreig, S.; Svensson, R. U.; Mamer, O. A.; Avizonis, D.; Shackelford, D. B.; Shaw, R. J.; Jones, R. G. *Proc. Natl. Acad. Sci. U. S. A.* **2014**, *111*, 2554–2559.
- (17) Wu, Z.; Li, D.; Zeng, F.; Tong, Q.; Zheng, Y.; Liu, J.; Zhou, Q.; Li, X.-N.; Chen, C.; Lai, Y.; Zhu, H.; Zhang, Y. *Phytochemistry* **2018**, *156*, 159–166.
- (18) Puri, A. W.; Mevers, E.; Ramadhar, T. R.; Petras, D.; Liu, D.; Piel, J.; Dorrestein, P. C.; Greenberg, E. P.; Lidstrom, M. E.; Clardy, J. *J. Am. Chem. Soc.* **2018**, *140*, 2002–2006.
- (19) Ehmann, D. E.; Trauger, J. W.; Stachelhaus, T.; Walsh, C. T. *Chem. Biol.* **2000**, *7*, 765–772.
- (20) Cassidy, P. J.; Albers-Schonberg, G.; Goegelman, R. T.; Miller, T.; Arison, B.; Stapley, E. O.; Birnbaum, J. *J. Antibiot.* **1981**, *34*, 637–648.
- (21) Poza, J. J.; Fernandez, R.; Reyes, F.; Rodriguez, J.; Jimenez, C. J. *Org. Chem.* **2008**, *73*, 7978–7984.